

On the Mechanical Behavior of Additively Manufactured Asymmetric Honeycombs

Lucas Casanova¹, Vineeth Vijayan Anitha¹, Nikhil Kadway¹, Arpit Gandhi¹, Thao Le¹,
Christine Lee², Dhruv Bhate¹

¹Ira A. Fulton Schools of Engineering, Arizona State University, Mesa, AZ 85212

²Herberger Institute of Design and Arts, Arizona State University, Tempe, AZ 85287

Abstract

From a design perspective, there are four decisions that need to be made when integrating cellular materials such as lattices and honeycombs into a structure: selection of the unit cell type, distribution of the size of the cells across the structure, optimization of individual cell walls/struts and junction thicknesses, and finally, integration of the cellular material with the outer form of the larger structure it is a part of. In this paper, we explore an alternative approach to designing cellular materials, borrowing concepts of symmetry from mathematics and the arts to manipulate 2-dimensional square honeycombs of uniform thickness, starting from a regular, periodic square, gradually varying symmetry and the number of shapes to create a range of forms. We report results of compression testing of specimens made with the Fused Deposition Modeling process, and study the effective specific properties of the honeycombs with regard to their peak stress at failure, densification strain and energy absorption. We report weak to no correlation to the first two of these, but demonstrate how asymmetry and negative space may be leveraged to formulate design principles for energy absorption.

Introduction

When it comes to incorporating cellular material designs into structures, there are four main questions a designer needs to address, demonstrated visually in Figures 1 (a) to (d).

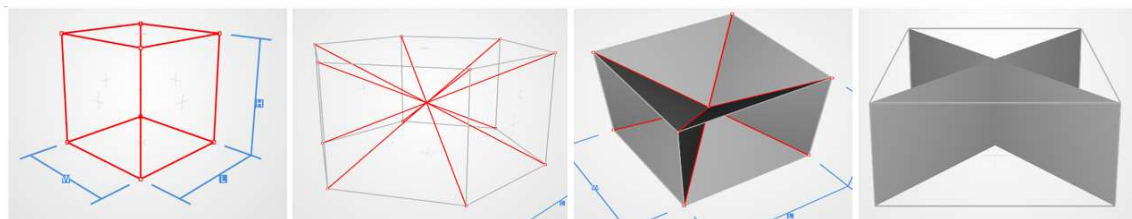
- What specific unit cell(s) should be selected?
- How should the size of these cells vary spatially?
- What are the optimal cell parameters?
- How best should the cells be integrated with the larger form of the structure?

The majority of the literature on cellular material design is primarily focused on the first question, namely that of unit cell selection. Cell selection is traditionally informed by different methods: an application of Maxwell's stability criterion to identify whether the structure is bending or stretch dominated [1], or derived from empirically observed behavior of cell shapes either computationally or experimentally, resulting in relationships termed as scaling laws [2]–[4]. A biomimetic approach may also be taken to cell selection, provided a clear structure-function relationship can be established and validated [5]. Design metrics such as material indices popularized by Ashby [6] and the geometric efficiency index [7] may also be used to numerically select between different shapes.

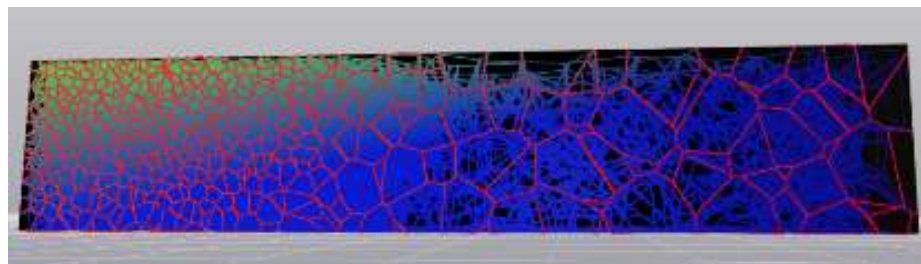
With regard to cell size distribution and parameter optimization, this is commonly treated in the context of relative density [2] where size and thickness of members such as walls and struts

can be modulated to achieve a certain desired density. Member parameter optimization is increasingly shifting to the computational domain however, with simulation being used to optimize parameters locally, as shown in Figure 1 (c).

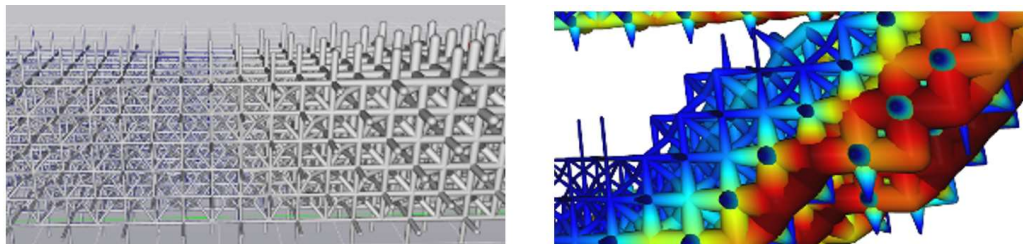
Finally, integration of cellular materials into a structure is currently primarily at the designers discretion, aided by design rules such as minimum skin thickness or dimensional specifications on outer form, that are application specific.



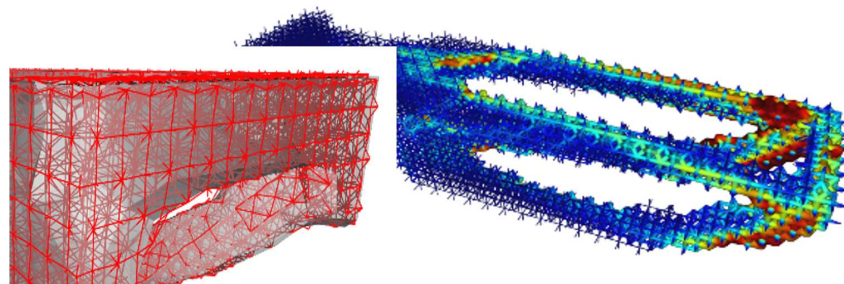
(a)



(b)



(c)



(d)

Figure 1. Examples of some of the considerations in the design of structures with cellular materials: (a) Unit cell shape selection, (b) Distribution of the size of these cells spatially, (c) Optimization of cell parameters such as thickness and (d) Integration of the cellular structure with skin, or into a topologically optimized form (all screenshots from the nTopology Element software [8])

In this paper, we present an alternative way of addressing the first two questions and examine its effectiveness for a very specific case of 2D honeycombs based on a regular square pattern. Instead of formulating the response to the questions of unit cell shape and size distribution in terms of their mechanics, we examine these questions in the context of mathematics and art, specifically the role of geometric symmetry in these fields. In the next section, we discuss why such an approach may be beneficial, before establishing the research questions we sought to answer in our work. This is then followed by a discussion of the design approach and manufacturing and testing methods we used. Finally, experimental results are discussed along with the conclusions that can be drawn from this exploratory work.

Motivation: Why Asymmetry?

Our motivation for studying asymmetry has its origins in observations made regarding the failure of regular cellular materials in previous work [9], [10]. As shown in Figure 2 (a) for a hexagonal honeycomb structure made of a polymer (ABS), failure under compression initiates via plastic hinging in a diagonal beam under bending, but is then quickly propagated at a 30 degree angle to neighboring cells that lie along that angle, as shown in Figure 2 (b) using both a 2D plane strain Finite Element Analysis model as well as experimentally observed.

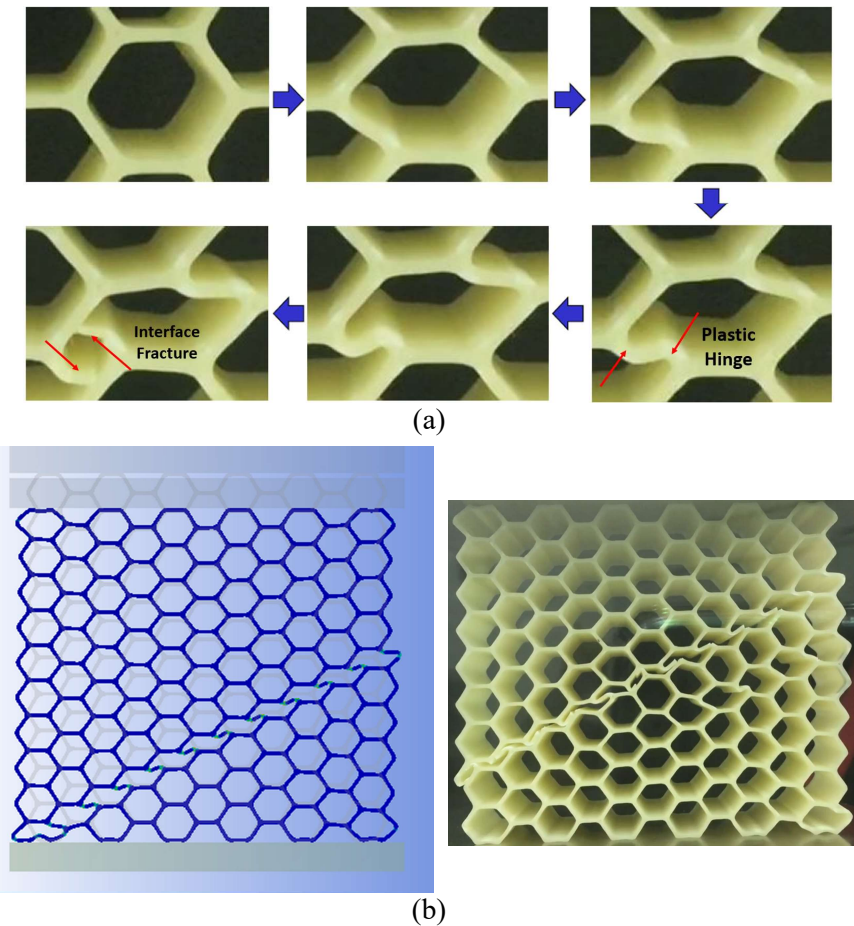


Figure 2. (a) Failure in a polymer hexagonal honeycomb initiates through the formation of a plastic hinge, followed by (b) a collapse of adjacent cells along a 30 degree angle

These studies raise the question of the role of symmetry in the response of honeycombs, and cellular materials more generally, particularly in the progression of failure through the structure, once initiated at a particular location. For the hexagonal honeycomb, for example, a question could be asked whether a local variation in shape or size would arrest the propagation of the failure mechanism and delay collapse of the structure. To address this question more systematically, we need to gain a better understanding of the meaning of symmetry, with regard to repeating patterns that we use in cellular materials.

Symmetry has been a key feature of study in mathematics [11], [12], nature [13] and art [14]–[16]. While a detailed understanding of each is beyond scope of this work, we present here some lines of thinking that influenced our choice of designs discussed in subsequent sections. Mathematicians define symmetry such that an object is invariant to any of various transformations such as rotation, reflection or scaling. Seventeen such transformations of symmetry have been identified [11], some of which are indicated in Figure 3.

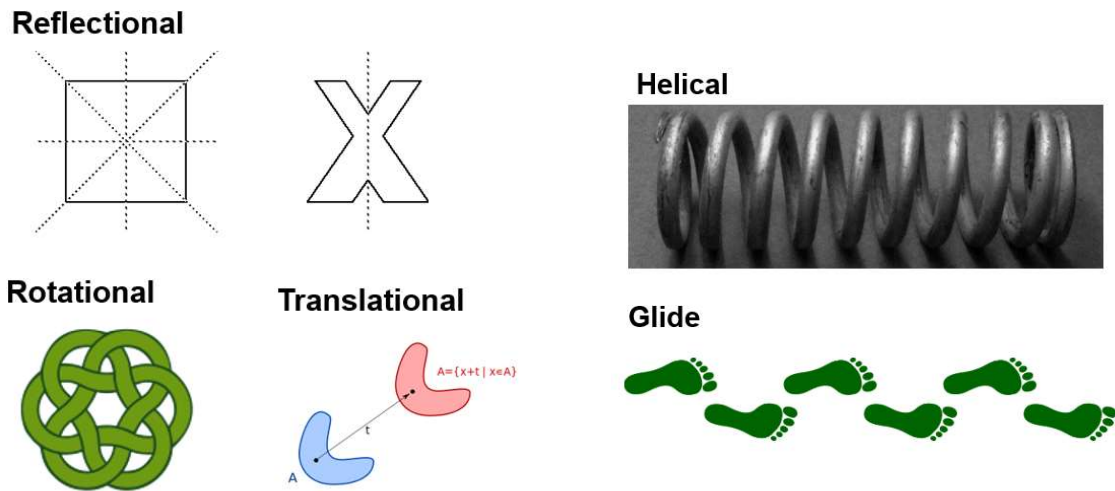


Figure 3. A selection of some forms of symmetry in mathematics (Attribution: Wikimedia commons, public domain)

Nature demonstrates symmetry in several ways – with regard to cellular materials, generally speaking, structures either have regular, repeating cells (with some variance) for reasons of storage, as shown in Figure 4 (a) for the nests of social insects, or can have asymmetric cells as seen in several radiolarian and in the venation patterns of insect wings, as shown in Figure 4 (b). While these cellular structures often have non-structural functions such as fluid transport or storage, it is likely that they represent structurally optimal solutions as well. In the case of the insect wings, for example, it has been suggested that the venation pattern increases the wing’s resilience to fracture [17]. The interesting question for our purposes is what is the benefit, if any, of asymmetry in natural cellular materials? While we don’t aim to address this question in this work, we hypothesize that the existence of asymmetry is indicative of the likelihood that such a benefit exists.

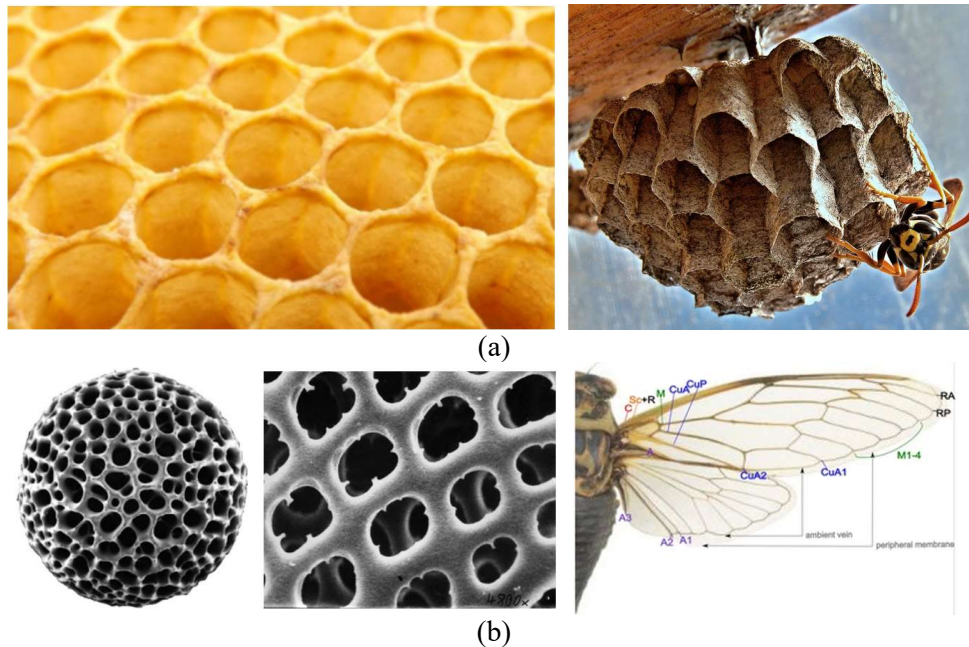


Figure 4. (a) Nests of social insects show a higher level of regularity, perhaps due to their storage function. (b) When storage is not a desired function, natural cellular structures tend to take on a range of asymmetric shapes as shown by radiolarian (Attribution: Hannes Grobe/AWI and Andreas Drews, Wikimedia Commons) and insect wings (above shown for a cicada wing, attribution: Bugboy 52.40, Wikimedia Commons)

Symmetry is a key element in art and design as well, particularly in the context of design that has a structural context. To quote the artist Wucius Wong [14], “*Sometimes a designer may prefer a visible structure. This means that the structural lines exist as actual and visible lines of desired thickness. Such lines should be treated as a special kind of unit form because they possess all the visible elements and can interact with the unit forms and the space contained by each of the structural subdivisions.*” Wong also discusses the notion of a “repetition structure”, when these unit forms are positioned regularly, and a “multiple repetition structure,” when there is more than one kind of structural subdivision that repeats in both shape and size. In mathematics, these are referred to as tessellations, some examples of which are demonstrated in Figure 5.

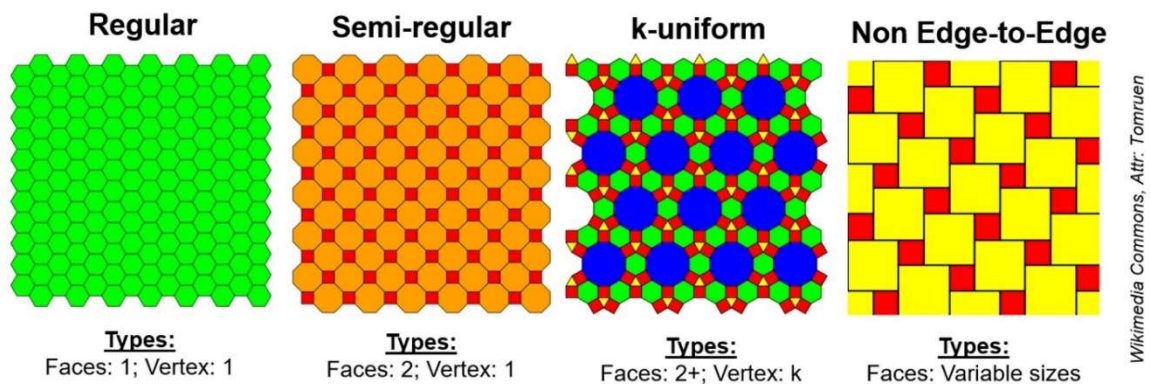


Figure 5. A selection of two-dimensional tessellation schemes (Wikimedia Commons Attribution – Tomruen, following [12])

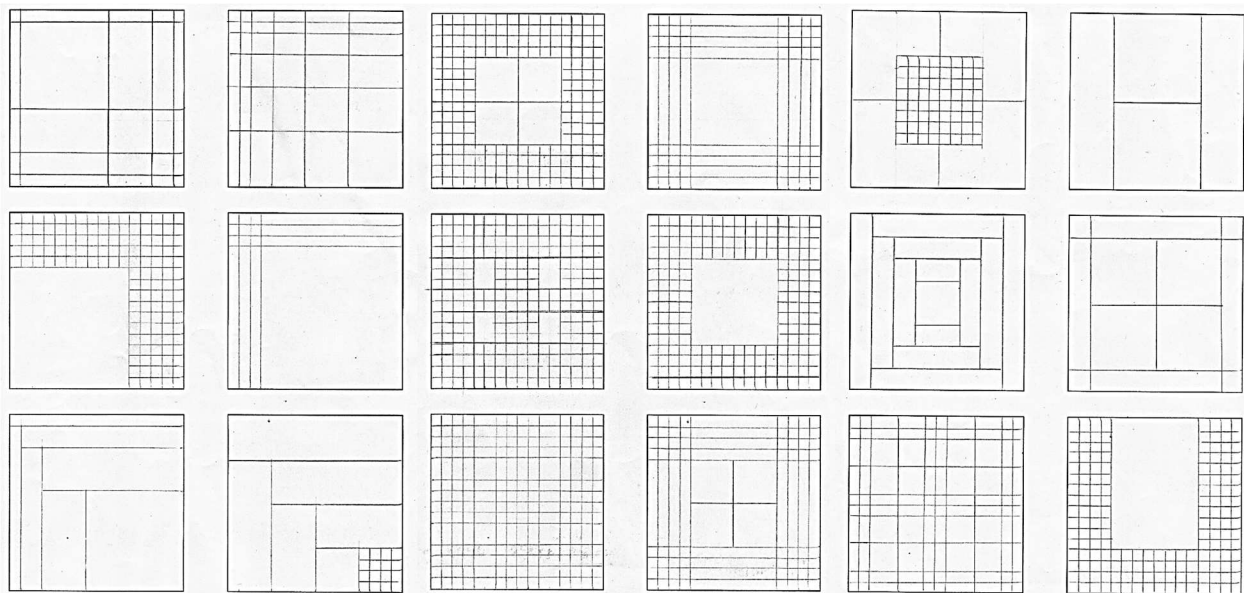
The preceding discussion suggests empirically and through an observation of natural structures, that there may be an inherent advantage to working with varying shapes and sizes. One of the possible ways of contextualizing this variation is in the language of symmetry, which as a subject has been widely explored in mathematics and art. The question for us in this work is whether we can leverage the framework of symmetry (or asymmetry) to identify what benefit it may bring us in the structural context when looking at mechanical behavior. To convert this abstract notion into a more tangible and actionable exploration, we formulate the following research questions:

- Is there a structural benefit to asymmetry or shape variance in cellular materials?
- Are there specific design principles that can be leveraged to maximize this benefit?

In this work, we seek to answer these questions within the context of two-dimensional honeycombs under compression, and examine the influence of asymmetry and the number of shapes (or “unit forms,” to use Wong’s term) on peak load at the onset of failure, the strain at densification and the energy absorbed (these terms will be defined more clearly in the following sections).

Design Approach

To make our work tractable, we decided to use as our base pattern a regular square honeycomb, and introduce asymmetry and shapes through a process of beam deletion. In the first step, we developed concept sketches on paper, some of which are shown in Figure 6. In order to classify these different forms, we decided to focus on two aspects: degree of symmetry and number of shapes, as shown in Figure 7.



© Christine Lee, 2017

Figure 6. Concept sketches derived from a regular square pattern that formed the basis for CAD design of the honeycombs in the study

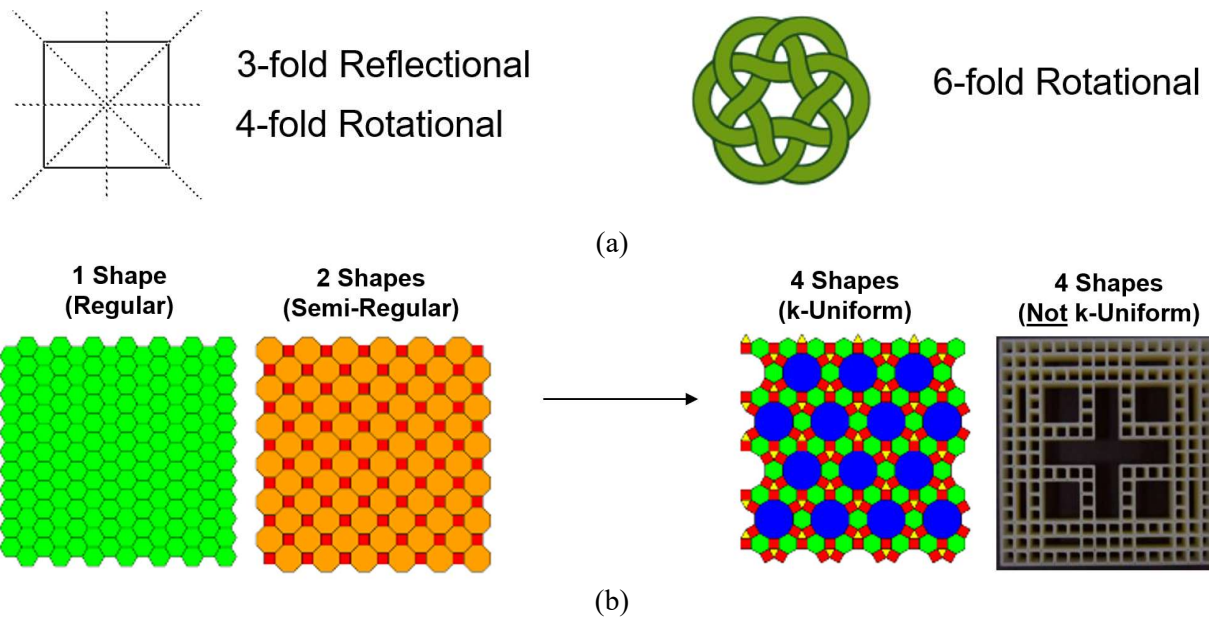


Figure 7. A classification scheme was developed to address two concepts: (a) degree of symmetry and (b) Number of shapes, or shape count (Wikimedia Commons Attribution – Tomruen, following [12])

The use of the terms degree of symmetry and shape count in the following discussion is not mathematically consistent, the aim is to provide a set of parameters that can be used to classify design and also assess how metrics of interest vary as a function of these parameters. Using this approach, a total of 23 2D honeycomb designs were created using CAD software. Two of these were considered as baseline honeycombs and have been fairly well described and characterized in the literature: the regular square pattern and the Voronoi pattern [18]. These patterns, as shown in Figure 8, can be considered to represent two extremes of symmetry and shape count, with the regular square pattern having local and global four-fold rotational and mirror symmetry and a shape count of 1, and the Voronoi having no symmetry due to its inherent stochastic nature and a shape count equal to the number of cells in the structure. All 23 honeycomb designs, including these two baselines are shown in Figure 8 which shows these designs as printed (discussed in the next section).

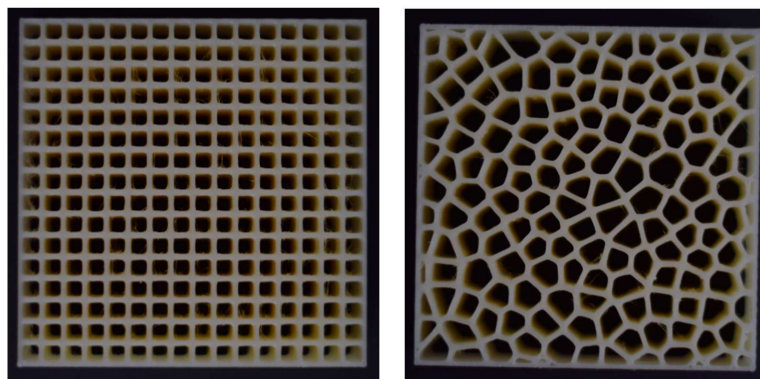


Figure 8. Square (left) and Voronoi (right) patterns, as representing two extreme ends of symmetry and shape count for this study

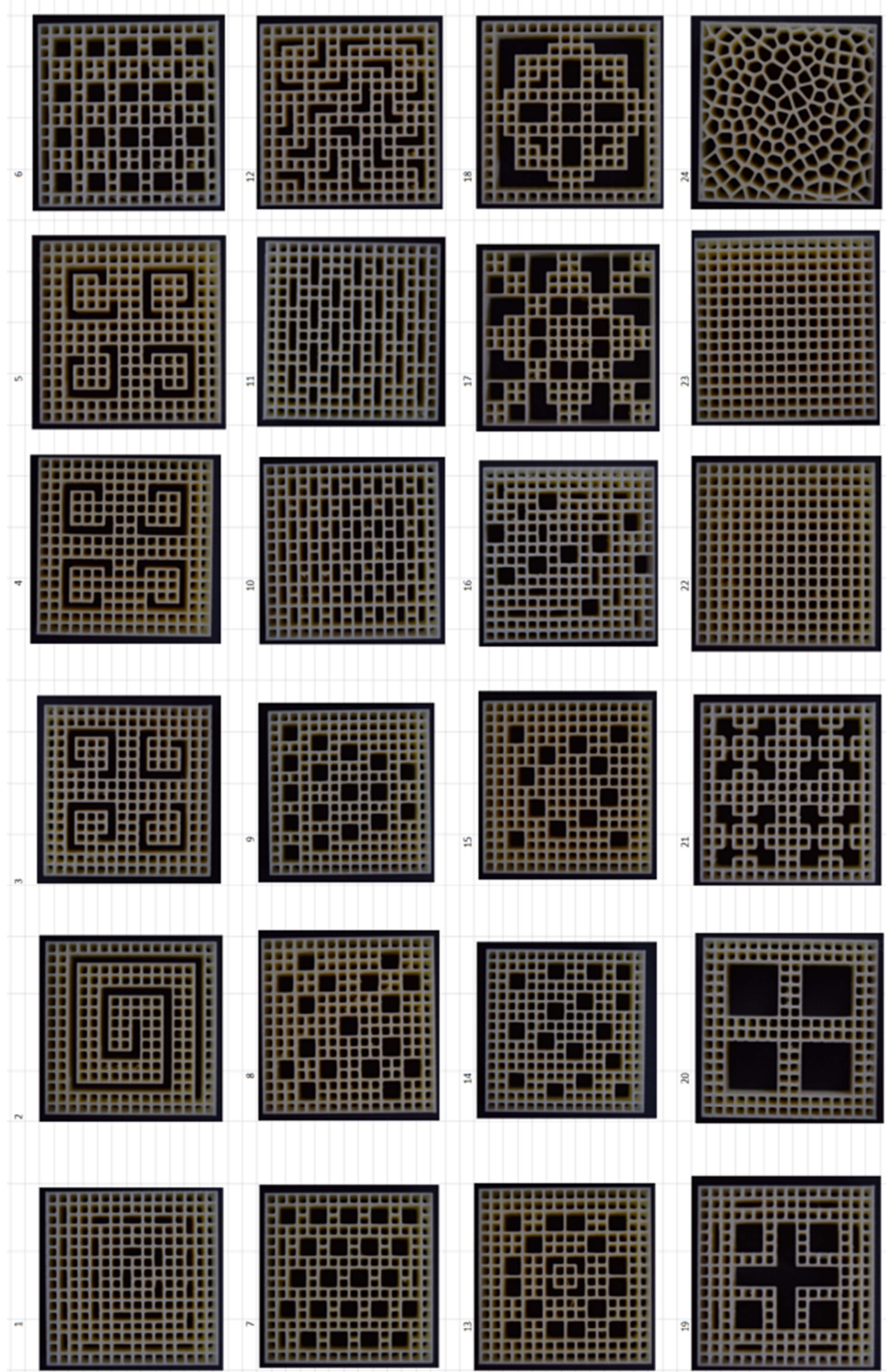


Figure 9. The 23 different designs (the baseline square was replicated) that were manufactured and tested in this work

Manufacturing and Test Methods

The designed honeycombs were manufactured using the Fused Deposition Modeling (FDM) process on a Stratasys Fortus™ 450mc. All honeycombs were set to a outer dimension of 2.91 inch x 2.91 inch square, with a 1 inch through thickness. The Voronoi honeycomb was slightly smaller (2.58 inch square) but this is corrected for in all stress-strain data represented here with a scaling factor. All honeycomb walls had a constant thickness of 0.032 inches. The parts were manufactured in ABS (Ivory) with a layer thickness of 0.010 inches and a contour width of 0.016 inches, which resulted in exactly two contours in the walls, following prior work [9]. All 23 specimens were printed in 2 successive builds – one regular baseline square honeycomb was printed in each build as a rough verification against drift from build-to-build.

The parts were tested under compression on an Instron 8801 machine with a 50kN load cell. Tests were run at an effective strain rate of 10^{-3} s^{-1} , following guidance of the ISO standard 13314 [19], though strictly speaking this was maintained as a constant velocity (displacement rate). The displacement rate was adjusted for the Voronoi specimen to account for its slightly shorter gauge length. A spherical seat was used in the load train to minimize errors with parallelism. Tests were conducted through densification, until peak load (50kN) was attained. Load-displacement data was obtained, which was then converted to effective stress and strain (representative of the honeycomb as opposed to the material). An example of the nature of the obtained results is shown in Figure 10, which was derived from compressing the regular square baseline honeycomb. This data was then used to estimate a failure stress (the highest stress value before the first reduction in stress), the strain at densification and finally, an energy density estimated as the area under the stress-strain curve, which itself was computed using a trapezoidal rule approximation. It is important to clarify that these effective stress and strain values are prone to errors on account of size effects [9]. In this work we are assessing not the property of a specific shape, but the response of the structure as a whole. All three metrics are demonstrated relative to the graph shown in Figure 10 and are the figures of merit used in subsequent discussion. A digital SLR camera was used to obtain high resolution video of the deformation process with each test lasting between 10-15 minutes – Video 1 shows the compression test for a regular square corresponding to Figure 10.

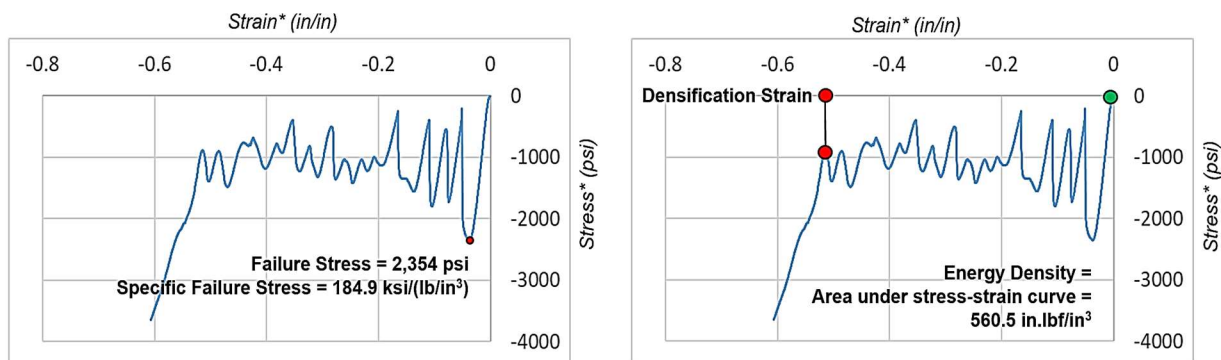
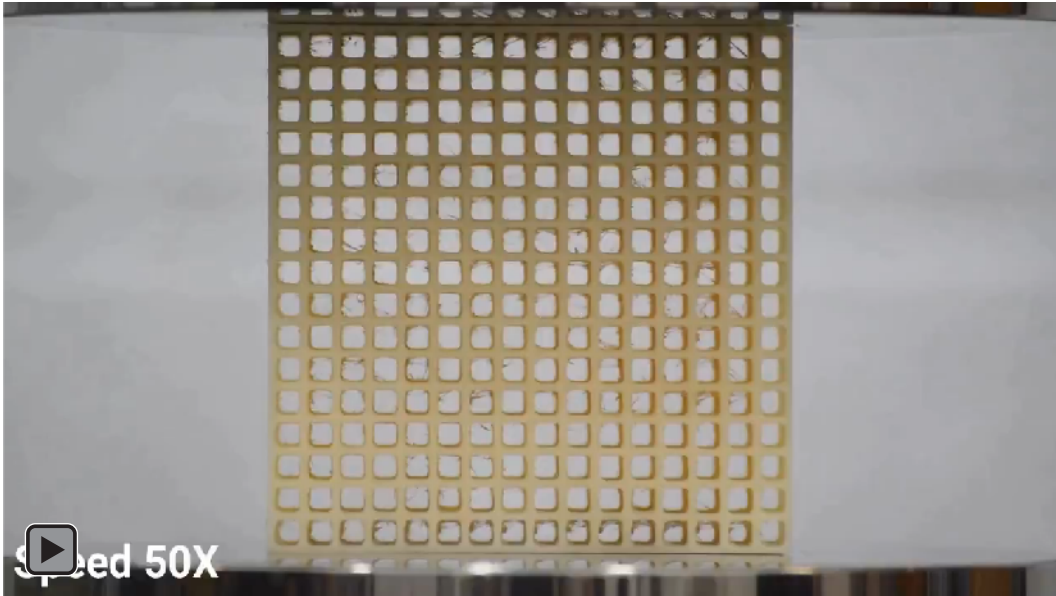


Figure 10. Effective stress-strain plots obtained from compression of a regular square honeycomb (shown in Figure 8), indicating the three metrics of interest in this work: failure stress, densification strain and energy density



Video 1. Compression of a square honeycomb (sped up 50 times), corresponding load displacement data in Figure 11.

As can be seen in Video 1, the square honeycomb fails by complete collapse of a row at a time. The collapse of a row is indicated by a drop in the load in Figures 11 (a) and (b), at which point it reaches a valley and starts to rise again till the next row collapses. This trend continues till there are no rows left to collapse, at which point we see the onset of densification.

Results

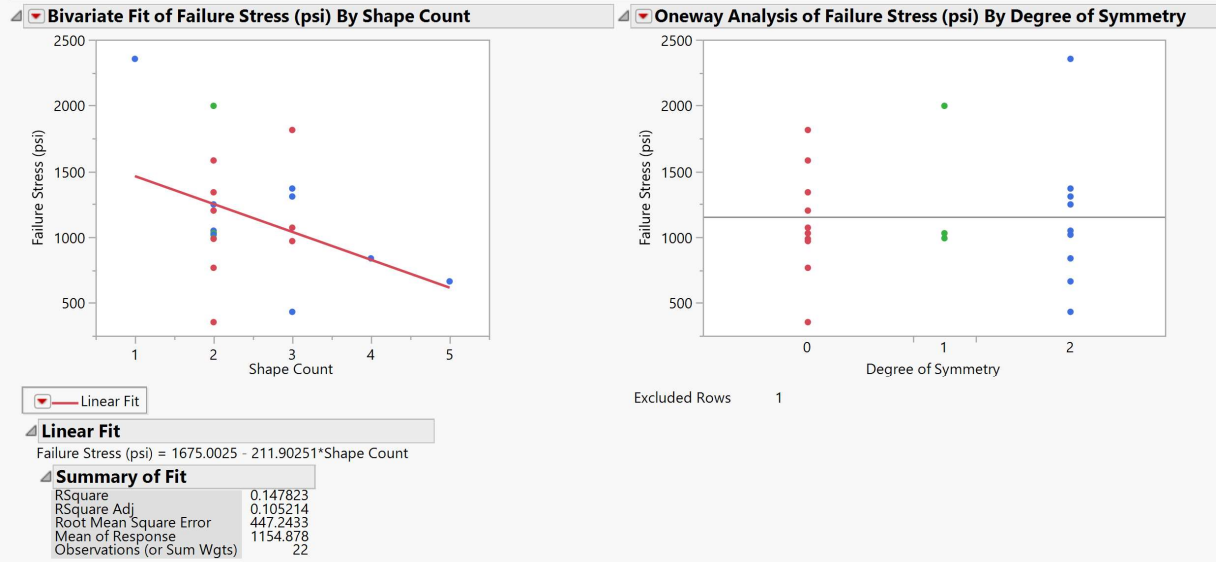
Twenty-one of the 23 specimens (excluding the replicated regular square patterns and the Voronoi pattern) were classified according to their degree of symmetry (0: low, 1: medium and 2: high) and into shape count, or number of shapes, ranging from 1-5. The Voronoi form was excluded from this classification any correlation studies but otherwise retained in the dataset. The order of symmetry selection as 0, 1 and 2 was determined in the following manner: structures that had no evident symmetry were placed in the 0 group and structures with 4-fold rotational symmetry in group 2. Shapes with symmetries between those two extremes were placed in group 1. All data obtained as shown in Figure 10 is listed in table 1 for all 24 specimens tested.

Correlation studies were conducted relating the three metrics of interest to the degree of symmetry and the shape count, and are plotted in Figures 11 (a) – (c). As can be seen in these plots, there are no correlations between symmetry and any of the variables, and there is weak correlation between shape count and the failure stress ($R^2 = 0.15$) and shape count and energy density ($R^2 = 0.22$). This dataset suggests symmetry by itself is not a relevant factor for the metrics of interest, at least for the range of structures studied here. On the other hand, the weak correlation of shape count with failure stress and energy density is suggestive of further investigation. Unfortunately only two data points exist for structures with shape counts greater than 4.

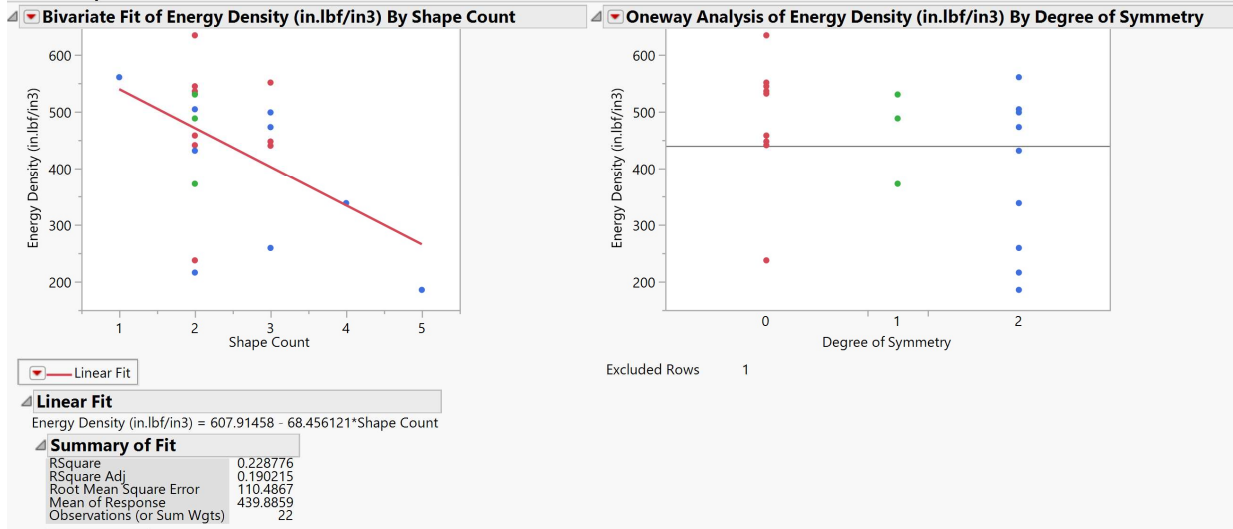
Table 1. Estimated values of failure stress, energy density and densification strain for all 24 specimens tested, along with shape count, degree of symmetry and volume fractions

Specimen #	Symmetry	Shape Count	Degree of Symmetry	Volume Fraction	Failure Stress (psi)	Energy Density (in.lbf/in ³)	Densification Strain
1	Spiral None	2	0	0.3250	1581.88	531.73	0.543
2	Spiral None	2	0	0.2981	353.45	458.06	0.600
3	Spiral (4)	2	0	0.3099	986.42	544.63	0.625
4	Spiral (4) 2-Rotational	2	1	0.3099	991.05	488.07	0.631
5	Spiral None	2	0	0.3099	1029.14	535.90	0.589
6	4-Rotational	3	2	0.2818	1368.60	472.84	0.605
7	None	3	0	0.2854	969.06	447.55	0.672
8	4-Rotational	2	2	0.2989	1247.98	504.21	0.599
9	1-Reflectional	2	1	0.2989	1028.95	371.94	0.616
10	2-Rotational	2	1	0.3116	1996.94	530.13	0.540
11	None	3	0	0.3132	1813.56	551.10	0.621
12	None	2	0	0.3054	766.29	237.27	0.492
13	4-Rotational	3	2	0.2968	1308.10	498.67	0.570
14	None	2	0	0.3012	1201.36	441.06	0.559
15	None	2	0	0.3107	1340.20	634.09	0.650
16	None	3	0	0.3110	1071.34	440.16	0.527
17	4-Rotational	3	2	0.2393	431.69	259.09	0.650
18	4-Rotational	5	2	0.2585	663.21	185.43	0.555
19	4-Rotational	4	2	0.2701	837.98	337.85	0.631
20	4-Rotational	2	2	0.2418	1017.60	215.85	0.575
21	4-Rotational	2	2	0.2834	1048.53	431.36	0.624
22	4-Rotational	Regular	2	0.3389	2354.00	560.50	0.510
23	4-Rotational	Regular		0.3389	2319.24	687.87	0.499
24	Voronoi	5	0	0.3049	670.40	402.04	0.661

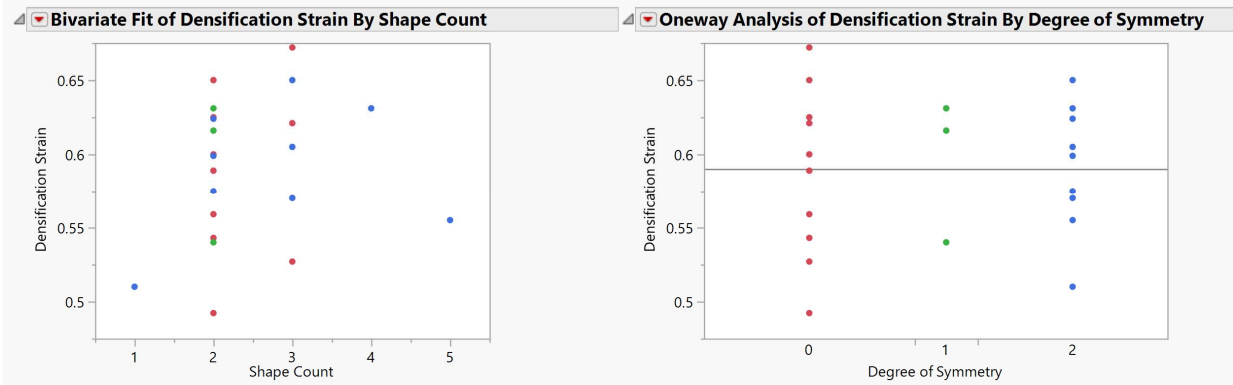
An important metric in the design of energy absorption structures such as crumple zones and helmets is the energy density as a function of the maximum transmitted stress [20], [21]. An ideal energy absorption device is able to absorb a lot of energy while keeping the maximum transmitted stress low. While the correlation between the two terms independently in this study is weak, it is worthwhile to examine their inter-relationship in the context of energy absorption. The two variables are plotted for all 24 shapes in Figure 12. The baseline square and Voronoi patterns are also identified. The first observation in this plot is the linear trend consistent with expectations and others in the literature – greater the failure stress, greater is the energy absorption. Densification strains are color coded since generally speaking, the higher the densification strain, the higher the energy absorption.



(a)



(b)



(c)

Figure 11. Correlation plots for shape count and degree of symmetry for (a) Failure stress, (b) Energy density and (c) Shape count

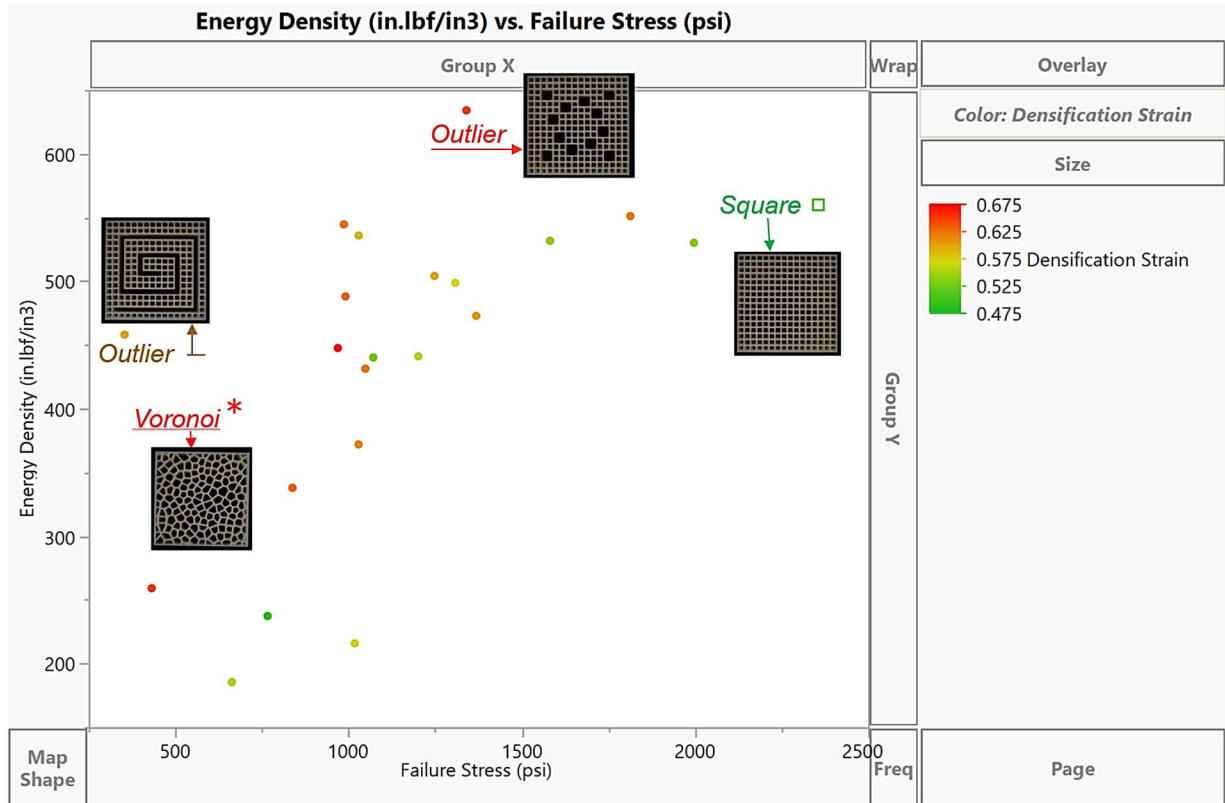


Figure 12. Correlation plots for shape count and degree of symmetry for (a) Failure stress, (b) Energy density and (c) Shape count. The colors correspond to the densification strains.

The two outliers in Figure 12 are worthy of further investigation. One of these is based on a spiral design and has an energy density similar to the regular square baseline, but at very low failure stresses. The other is a structure consisting of two square shapes and has the highest energy density of all 24 specimens considered, at a failure stress about half of the regular square pattern. A closer inspection of these shapes may reveal the mechanism behind their behavior.

The compression load-displacement response of the spiral pattern in relationship to the square pattern is shown in Figure 13. Remarkably, the spiral pattern manages to keep peak stress to less than half that for the square pattern to about 45% strain and only exceeds the peak stress of the square pattern at densification. Compression of the spiral pattern is demonstrated in Video 2. The best way to interpret this shape may be to invoke the notions of positive and negative space as defined and used by artists. To quote Wong [14], “*Sometimes a designer may prefer a visible structure. This means that the structural lines exist as actual and visible lines of desired thickness. Such lines should be treated as a special kind of unit form because they possess all the visible elements and can interact with the unit forms and the space contained by each of the structural subdivisions. Visible structural lines can be positive or negative. When negative, they are united with negative space or negative unit forms, and they can cross over positive space or positive unit forms. Negative structural lines are considered as visible because they have a definite thickness which can be seen and measured.*”

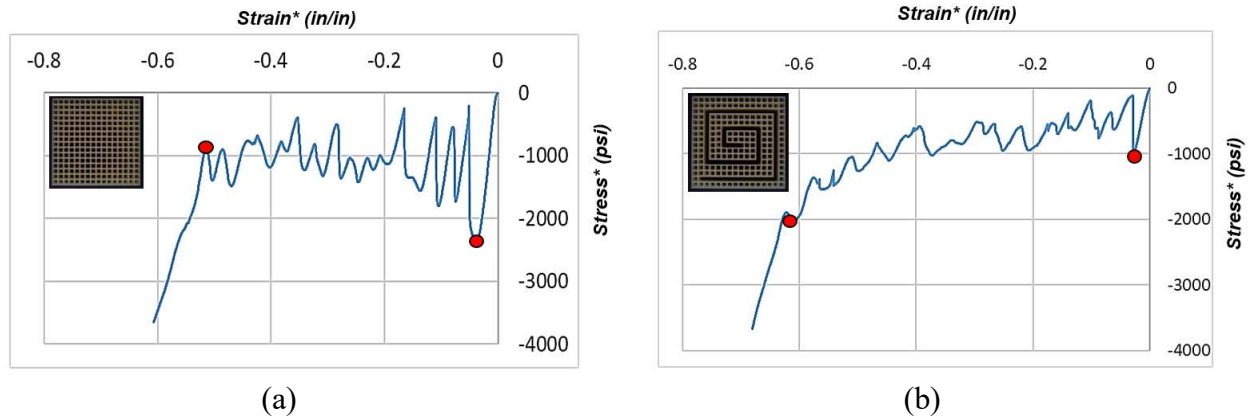
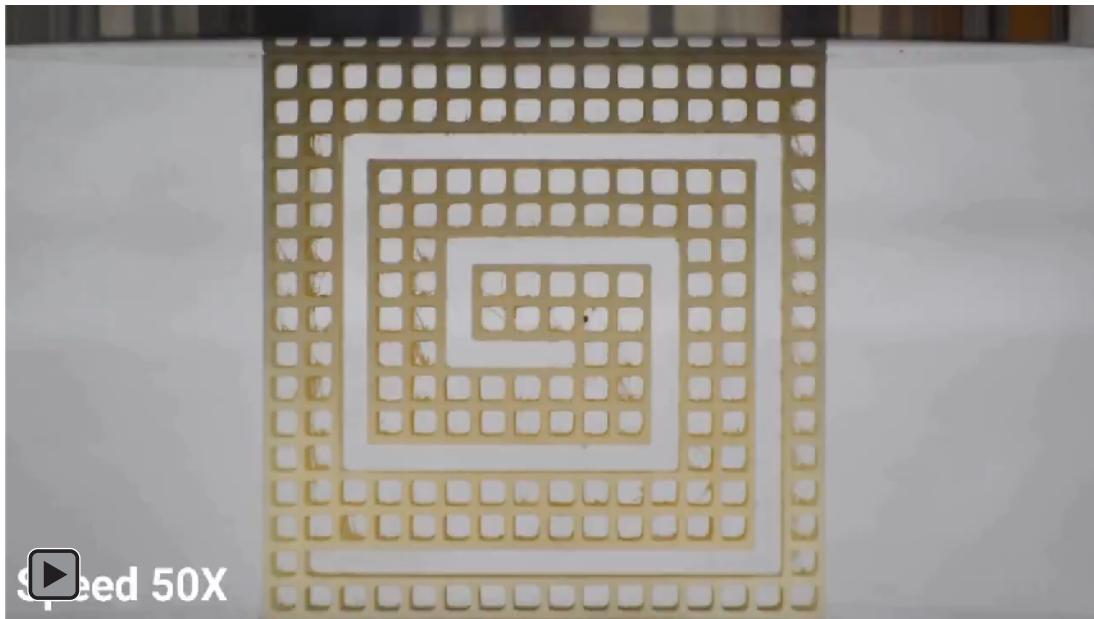


Figure 13. Effective stress-strain plots for (a) the regular square baseline and (b) the spiral shape – the spiral shape shows very low failure stress and a gradual increase in stress to densification



Video 2. Compression of a honeycomb with a spiral pattern (sped up 50 times), corresponding load displacement data in Figure 13 (b).

The spiral pattern under compression thus makes use of negative space to diminish the increase in stress – and the presence of a spiral extends the time before densification (unlike in the regular square pattern where load is merely transferred from one failed row to the next). The strain at densification is also extended since the negative space in the spiral is consumed first before negative space within each of the square unit cells/forms is consumed. Further evaluation work into the use of spiral negative space in energy absorption devices is recommended based on these findings.

The second outlier shape of interest in Figure 12 was realized by a strategy of deleting beams to create a structure consisting of two square unit cell shapes. The larger squares were randomly created within the square pattern, and have no rotational symmetry. This shape has the

highest energy density of all designs evaluated but at a failure stress approximately half that of the regular square pattern, as seen in the comparison in Figure 14.

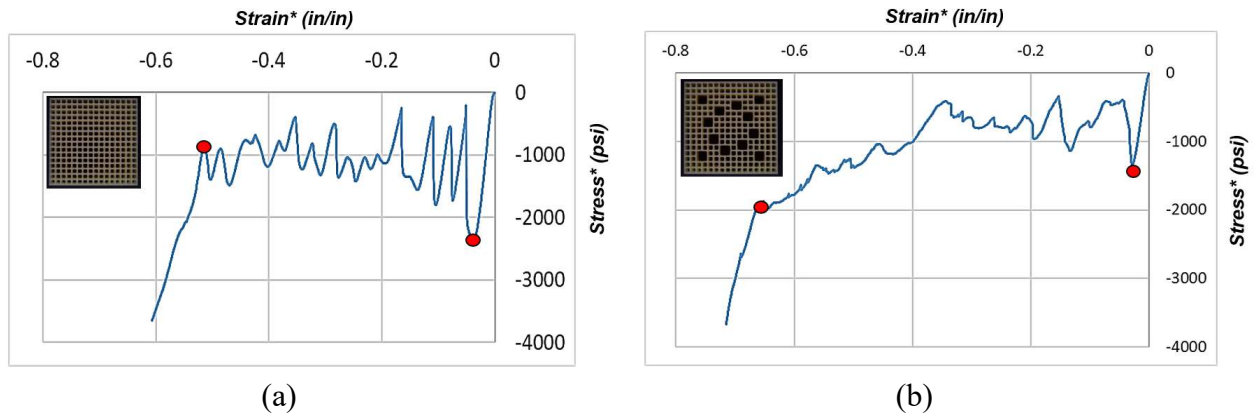
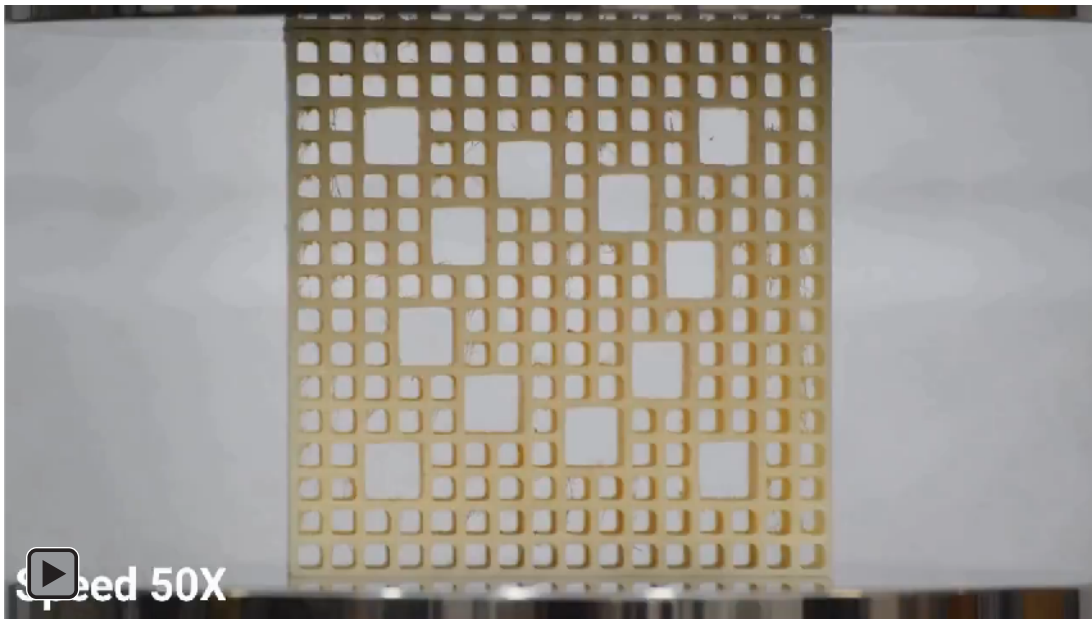


Figure 14. Effective stress-strain plots for (a) the regular square baseline and (b) the asymmetric dual square shape – while the latter shows a higher stress (compared to the spiral shape in Figure 13 (b)), densification sets in later and the stress increase to densification is also at higher values, resulting in higher net energy density.



Video 3. Compression of a honeycomb with an asymmetric dual-square shape form (sped up 50 times), corresponding load displacement data in Figure 14 (b).

An examination of Video 3 reveals a similar mechanism at play as in the spiral pattern. Negative space serves to reduce the peak stress of the regular square but the lack of connectivity of this space does not make it as effective as the spiral pattern. On the other hand, the structure is able to provide more resistance to the load than the spiral pattern and therefore has a higher energy density. In one sense, it may be said that this asymmetric dual-square pattern represents a design between the connected negative space of the spiral and the resistance of the regular square pattern.

Discussion

A question remains as to why the other dual-square shapes, of which there were four in this work, did not behave similar to the structure in Video 3. As shown in Figure 15, only one of these four patterns fell outside the cluster of data points, the others seemingly not providing any exceptional benefit. We can say with some confidence that creation of negative space by removing material has the net effect of lowering the peak stress. This is evident since the pattern with the highest failure stress is the regular square. It is more challenging to explain why there is such a large difference in shapes that follow the similar strategy with regard to the number of shapes.

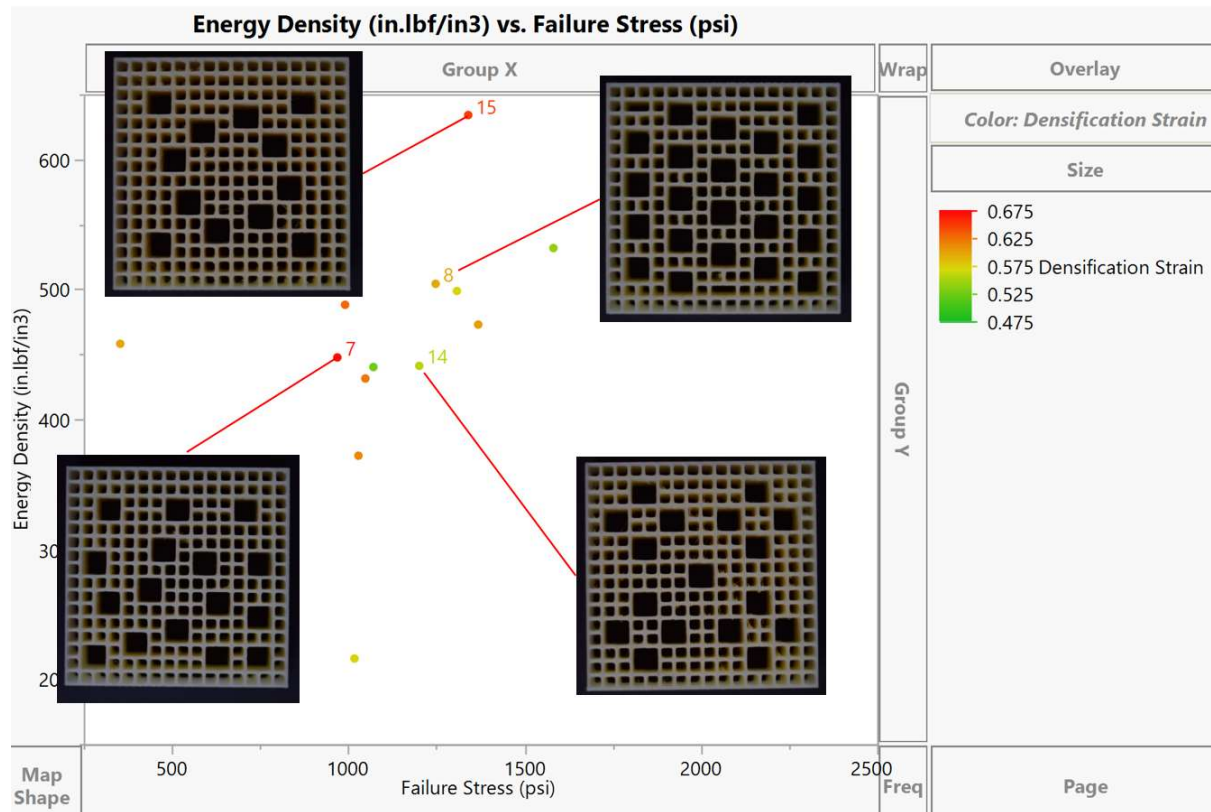


Figure 15. Dual-square shapes are not all alike. The essential idea of two square shapes was incorporated into four different shapes with varying energy densities.

An explanation for this behavior may be developed based on an examination of the effective stress-strain curves for all four shapes, as shown in Figure 16, where the red curve represents the outlier and the blue curves represent the other three patterns. Interestingly, they all have the similar failure stress values. With regard to strain at densification, the outlier is in between the other three shapes. This rules out failure stress and densification strain as the only, or indeed primary reasons for this difference in energy density. It appears that the higher energy density for the outlier pattern is on account of the increase in stress after about 40% strain at a pace faster than the others and held to a relatively high densification strain.

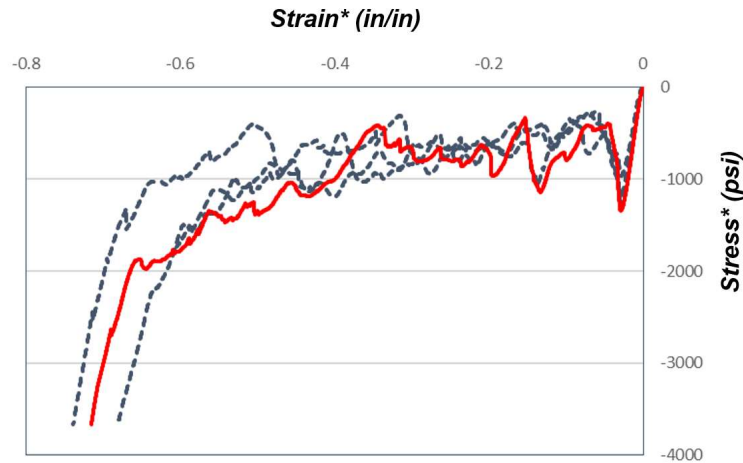


Figure 16. Effective stress-strain curves for the four shapes in Figure 15, the red curve represents the outlier with respect to energy density, the dashed blue curves represent the three other patterns

One possible explanation for this difference follows from Figure 17, where lines are drawn connecting empty, large square cells that lie normal to the axis of compression. As can be seen in Video 4, rows with two or more large empty squares collapse first, crushing the smaller squares in the vicinity and then shifting the load to the next row with two or more large squares in it. However, if we wish to increase the energy absorption, every increase in strain must be at a relatively high stress level (but lower than the allowable maximum). The outlier has only two pairs of large squares in the same row, resulting in a stiffer collapse of the large squares. The other structures have four or more rows of these collinear large squares, which may explain why they accumulate large strains but at lower stress levels, resulting in lower energy absorption. An improved design may be obtained with squares staggered such that no two large squares occur in the same line.

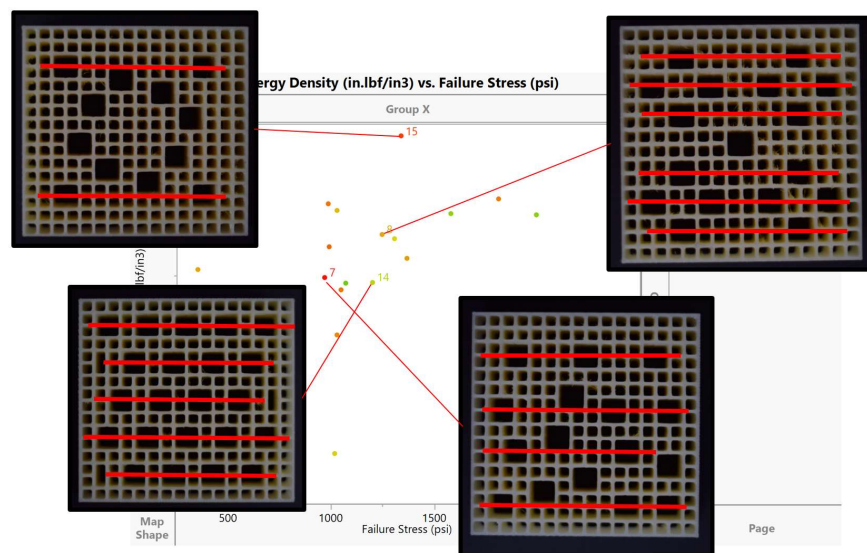
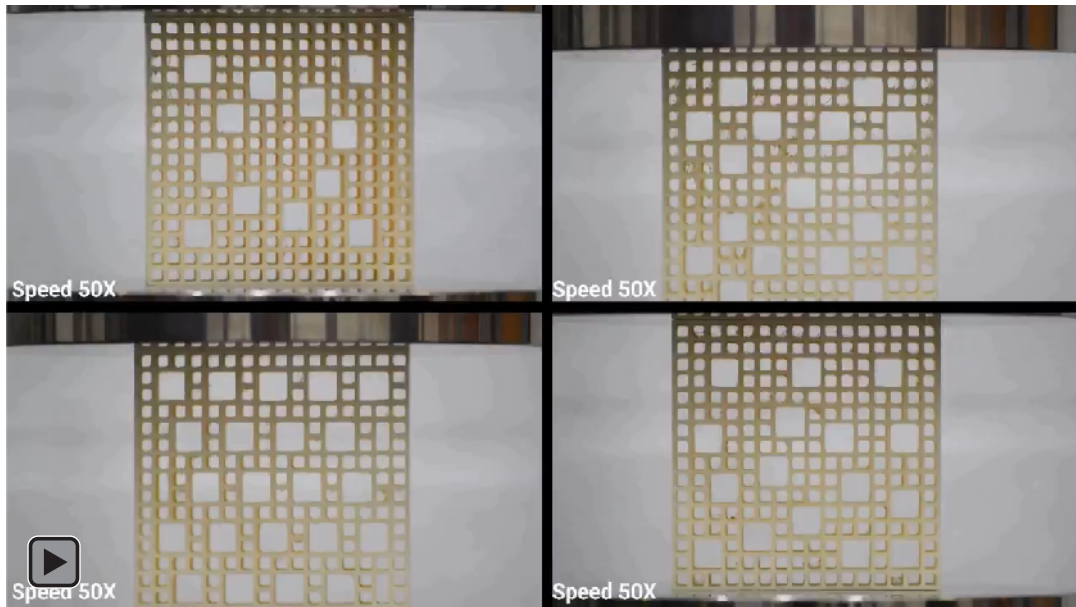


Figure 17. A hypothesis based on load transfer paths to explain why structures made of the same shapes have variable response. The red lines indicate locations of two or more large squares (made of deleted beams) that lie in the same load path when under compression.



Video 4. Compression of four different dual-square shape patterns (sped up 50 times), corresponding to the shapes shown in Figure 15.

Conclusions

The work described in this paper set out to establish whether symmetry and/or the number of shapes influenced behavior of 2D honeycombs under compression. While no strong correlation was found for failure stress, energy absorbed or strain at densification, an examination of the relationship between energy absorption and maximum stress revealed some interesting findings. The two following design rules are suggested as a result of this work. More data is needed to validate these findings:

- Connected negative spaces such as the spiral pattern can be employed to diminish the failure stresses in cellular materials. Spirals have an ability to allow continuous deformation at low stresses.
- Higher energy absorption at low maximum stress can be obtained through a staggered removal of beams such that collapsing structures are not collinear relative to the direction of loading

Thus, while not conclusive, our work suggests that the use of connected negative space and non-collinear material removal may have the potential to improve the energy absorption in cellular materials. More generally, it makes the case for studying cellular material design beyond the traditional notions of cell shape selection and relative densities as specified by cell size and/or parameter variation, and it is this that our future work will aim to explore.

References

- [1] V. S. Deshpande, M. F. Ashby, and N. A. Fleck, “Foam topology: Bending versus stretching dominated architectures,” *Acta Mater.*, vol. 49, no. 6, pp. 1035–1040, 2001.

- [2] L. J. Gibson and M. F. Ashby, *Cellular Solids: Structure and Properties*, 2nd ed. Cambridge Solid State Science Series, 1999.
- [3] M. F. Ashby, A. G. Evans, N. A. Fleck, L. J. Gibson, J. W. Hutchinson, and H. N. G. Wadley, *Metal Foams : A Design Guide*. Butterworth Heinemann, 2000.
- [4] M. R. O’Masta, L. Dong, L. St-Pierre, H. N. G. Wadley, and V. S. Deshpande, “The fracture toughness of octet-truss lattices,” *J. Mech. Phys. Solids*, vol. 98, no. April 2016, pp. 271–289, 2017.
- [5] T. McNulty *et al.*, “A Framework for the Design of Biomimetic Cellular Materials for Additive Manufacturing,” in *Solid Freeform Fabrication Symposium*, 2017, pp. 2188–2200.
- [6] M. F. Ashby, *Materials Selection in Mechanical Design*, Fourth. 2011.
- [7] J. B. Berger, H. N. G. Wadley, and R. M. McMeeking, “Mechanical metamaterials at the theoretical limit of isotropic elastic stiffness,” *Nature*, vol. 543, no. 7646, pp. 533–537, 2017.
- [8] NTopology, “Element.” 2018.
- [9] T. Le, D. Bhate, J. M. Parsey, and K. H. Hsu, “Determination of a Shape and Size Independent Material Modulus for Honeycomb Structures in Additive Manufacturing,” *Solid Free. Fabr. Symp.*, 2017.
- [10] R. Sharma *et al.*, “A Comparison of Modeling Methods for Predicting the Elastic-Plastic Response of Additively Manufactured Honeycomb Structures,” in *Solid Freeform Fabrication Symposium*, 2018.
- [11] M. Du Sautoy, *Symmetry : A Journey into the Patterns of Nature*. 2008.
- [12] D. Chavey, “Tilings by Regular Polygons - II A Catalog of Tilings,” *Comput. Math. Applic.*, vol. 17, no. 1–3, pp. 147–165, 1989.
- [13] F. T. Lewis, “A Note on Symmetry as a Factor in the Evolution of Plants and Animals Published by : The University of Chicago Press for The American Society of Naturalists Stable URL : <http://www.jstor.org/stable/2456531>,” *Am. Nat.*, vol. 57, no. 648, pp. 5–41, 1923.
- [14] W. Wong, *Principles of Form and Design*, 1st ed. Wiley, 1993.
- [15] C. Leborg, *Visual Grammar*, 1st ed. Princeton Architectural Press, 2006.
- [16] D. A. Dondis, *Primer of Visual Literacy*, Revised ed. MIT Press, 1973.
- [17] J. H. Dirks and D. Taylor, “Veins improve fracture toughness of insect wings,” *PLoS One*, vol. 7, no. 8, 2012.
- [18] I. Christodoulou and P. J. Tan, “Crack initiation and fracture toughness of random Voronoi honeycombs,” *Eng. Fract. Mech.*, vol. 104, pp. 140–161, 2013.
- [19] ISO, *ISO 13314: Mechanical testing of metals, ductility testing, compression test for porous and cellular metals*. 2011.
- [20] M. Mohsenizadeh, F. Gasbarri, M. Munther, A. Beheshti, and K. Davami, “Additively-manufactured lightweight Metamaterials for energy absorption,” *Mater. Des.*, vol. 139, pp. 521–530, 2018.
- [21] A. G. Evans, M. Y. He, V. S. Deshpande, J. W. Hutchinson, A. J. Jacobsen, and W. B. Carter, “Concepts for enhanced energy absorption using hollow micro-lattices,” *Int. J. Impact Eng.*, vol. 37, no. 9, pp. 947–959, 2010.